On the relationship between thermosphere density and solar wind parameters during intense geomagnetic storms

Jianpeng Guo,[1,2] Xueshang Feng,[1] Jeffrey M. Forbes,[3] Jiuhou Lei,[3] Jie Zhang,[4] and Chenming Tan[2]

Received 26 July 2010; revised 27 September 2010; accepted 13 October 2010; published 30 December 2010.

[1] Total mass density measurements at 72°S, 0°, and 72°N latitude from the CHAMP satellite near 400 km altitude are used to provide a quantitative assessment of the relationship between solar wind energy input and density variations during intense ($Dst \leq -100$ nT) geomagnetic storms that occurred between August 2001 and December 2006. Correlations between the thermosphere density variations and various solar wind parameters and coupling functions representing the energy input into the thermosphere reveal significantly different characteristics during different geomagnetic storms. Statistical analysis shows that, out of the chosen solar wind parameters including coupling functions, the Borovsky parameter correlates best with the global scale density variations. The correlations at the equator are significantly higher than those at high latitudes. Moreover, the correlations on the dayside are almost the same as those on the nightside at 72°S and 0° latitude, whereas the correlation on the nightside is slightly higher than that on the dayside at 72°N latitude. These results indicate that it might be possible to use solar wind measurements to improve predictions of thermosphere density perturbations and the resulting changes in satellite drag.

Citation: Guo, J., X. Feng, J. M. Forbes, J. Lei, J. Zhang, and C. Tan (2010), On the relationship between thermosphere density and solar wind parameters during intense geomagnetic storms, *J. Geophys. Res.*, *115*, A12335, doi:10.1029/2010JA015971.

1. Introduction

[2] A part of energy supplied to the magnetosphere from the solar wind is deposited in the high-latitude thermosphere via particle precipitation and Joule heating, which govern the structure and dynamics of the thermosphere. Some of this energy is redistributed through transport processes, which, in the case of storms, affect the thermosphere globally. According to *Wilson et al.* [2006], during storm times, short timescale (1–2 days) variations in the structure of the thermosphere are controlled by variations in magnetospheric energy inputs and not so much by variations in the solar EUV energy input [e.g., *Bowman and Tobiska*, 2006; *Tobiska et al.*, 2006; *Guo et al.*, 2007, 2008, and references therein]. Several manifestations of energy transformation and redistribution may combine to produce the disturbed state of the thermosphere. These manifestations are reviewed in detail by *Sutton et al.* [2009]. The relationship between geomagnetic disturbances and thermospheric composition, density, and winds has been studied in depth for decades [e.g., *Prölss*, 1980; *Forbes et al.*, 1987, 1993, 1996, 2005; *Liu and Lühr*, 2005; *Sutton et al.*, 2005; *Bruinsma et al.*, 2006; *Lei et al.*, 2010], but better empirical relationships are still needed to meet the needs of satellite orbit prediction and conjunction analyses.

[3] *Forbes et al.* [2005] examined the correlations between the thermosphere density variations and various solar wind parameters and geophysical indices representing precursors related to energy input into the thermosphere during the disturbed period of 15–24 April 2002. The densities were derived from the measurements by the accelerometer experiment on the CHAMP satellite. The results suggested that the global scale density variations are best correlated with the magnitude of the interplanetary magnetic field as measured by the ACE spacecraft. Although their results may be interesting and thought-provoking, it must be recognized that a 10 day interval does not represent a sufficiently large statistical sample to draw definitive conclusions; in fact, a vastly larger sample is necessary. This motivates the primary objective of the present study, to quantitatively characterize the large-scale response of thermospheric density to solar wind energy input during intense geomagnetic storms.

[4] At present, there are no direct observational means of determining the energy transfer from the solar wind to the magnetosphere and thermosphere-ionosphere system. In fact, we do not even know the details of how and where the transfer takes place. The need to have useful estimates of energy available for magnetospheric dynamics has led to the formulation of a large number of coupling functions [*Koskinen and Tanskanen*, 2002]. The different input parameters have

[1]SIGMA Weather Group, State Key Laboratory of Space Weather, CSSAR, Chinese Academy of Sciences, Beijing, China.
[2]Key Laboratory of Solar Activity, National Astronomical Observatories, Chinese Academy of Sciences, Beijing, China.
[3]Department of Aerospace Engineering Sciences, University of Colorado at Boulder, Boulder, Colorado, USA.
[4]Department of Computational and Data Sciences, George Mason University, Fairfax, Virginia, USA.

0148-0227/10/2010JA015971

been correlated with different ionospheric and magnetospheric indices or proxies of energy consumption. To find out the optimal solar wind parameters representing the energy input into the thermosphere during intense geomagnetic storms, correlations at different time lags are calculated between density variations and various solar wind parameters. The parameters examined include the magnetic field strength B, the Bz component, the solar wind velocity v, the dynamic pressure Pdy ($Pdy = nmv^2$, where n is proton density and m is mass), and the solar wind electric field Ey. Furthermore, it is interesting to investigate whether better correlations can be obtained by combining various solar wind parameters, such as the most widely used energy input function, the so-called epsilon parameter of *Akasofu* [1981]. Therefore, we further examined two types of solar wind-magnetosphere coupling functions, namely, the solar wind "driver function" and the solar wind "control function" [cf. *Borovsky*, 2008]. The driver functions are derived with "tuning" to optimize correlation coefficients between magnetospheric measurements and solar wind measurements, while there are no explicit free parameters in the control function.

[5] The solar wind driver functions used are the well-known Akasofu function (or the epsilon parameter) (equation (1)) [*Akasofu*, 1981] and the Newell formula (equation (2)) [*Newell et al.*, 2007],

$$\varepsilon(W) = \frac{4\pi}{\mu_0} vB^2 \sin^4\left(\frac{\theta}{2}\right) l_0^2, \tag{1}$$

$$d\Phi/dt = v^{4/3} B_T^{2/3} \sin^{8/3}\left(\frac{\theta}{2}\right). \tag{2}$$

[6] The variables v, B, B_T, θ, and l_0 on the right-hand side are given in SI units and denote the solar wind velocity, the solar wind magnetic field magnitude, the solar wind magnetic field perpendicular to the Sun-Earth line, the IMF clock angle, and the scaling factor, respectively. The scaling factor was empirically determined to be $l_0 = 7\ R_E$. It is scaled to numerically correspond to the estimated energy output in the magnetosphere and the physical dimension of power for the energy input rate [*Koskinen and Tanskanen*, 2002].

[7] The solar wind control function used is the Borovsky function [*Borovsky*, 2008], i.e., a reconnection rate written in terms of upstream solar wind parameters,

$$R = 0.4\mu_0^{1/2} \sin(\theta/2) \rho v^2 \left(1 + 0.5 M_{ms}^{-2}\right)(1+\beta_s)^{-1/2} \cdot \left[C\rho + (1+\beta_s)^{-1/2}\rho_m\right]^{-1/2} \left[(1+\beta_s)^{1/2} + 1\right]^{-1/2} \tag{3}$$

where β_s,

$$\beta_s = 3.2 \times 10^{-2} M_A^{1.92}, \tag{4}$$

is the plasma beta of the magnetosheath near the nose of the magnetosphere,

$$C = \{[1/4]^6 + [1/(1 + 1.38 \log_e(M_A))]^6\}^{-1/6} \tag{5}$$

is the compression ratio of the bow shock,

$$M_{ms} = v/((B/4\pi\rho) + 2P/\rho)^{1/2} \tag{6}$$

is the magnetosonic Mach number of the solar wind, and

$$M_A = v(4\pi\rho)^{1/2}/B \tag{7}$$

is the Alfvén Mach number of the solar wind. A term $\sin(\theta/2)$ is also added to account for the component reconnection when the IMF has a clock angle of θ. In these expressions v, ρ, B, and P are the speed, mass density, magnetic field strength, and particle pressure (thermal plus kinetic) in the upstream solar wind. In calculating the Borovsky function, we take $\rho_m = 0$ due to no information about the dayside magenospheric mass density ρ_m [see *Guo et al.*, 2010].

[8] Section 2 describes the data sets and analysis method used in this study. Section 3 presents examples of actual storm responses to reveal the differences among the correlations of different solar wind parameters and the density during intense ($Dst \leq -100$ nT) geomagnetic storms. It also discusses results of statistical analysis on the relationship between various solar wind parameters and density variations. Discussion and conclusions follow in section 4.

2. Data Analysis

[9] In this study, we use the total mass densities inferred from accelerometer measurements on the CHAMP satellite, which was launched into a near-circular orbit with an inclination of 87.3° on 15 July 2000 [*Reigber et al.*, 2002]. CHAMP provides near-global latitudinal coverage at an approximate altitude of 400 km in two local time sectors. The procedures currently used for density retrieval are described in detail by *Sutton* [2008], and the density data have been normalized to 400 km altitude and averaged into 3° latitude bins between ±87° geodetic latitude to reduce random errors. Density data of three latitude bins (72°S, 0°, and 72°N) are selected to study the density response to the solar wind energy input. To reduce the noise associated with traveling atmospheric disturbances and smooth the correlation results, the density data are further averaged along the orbit in 12° bins for each selected latitude region.

[10] This research focuses on the intense ($Dst \leq -100$ nT) geomagnetic storms that occurred between August 2001 and December 2006. Referring to *Zhang et al.* [2007, 2008], there are 52 solar interplanetary events that produced intense geomagnetic storms during this period. The corresponding solar wind magnetic field and plasma parameters are available from the 1 min averaged OMNI database (GSM coordinates at 1 AU). For each storm, a correlation analysis was done between the density and solar wind data after removing their mean values during the period starting at the onset of the storm and spanning 2.5 days. Generally, the time span of the response of thermosphere to the intense storm are between 2 and 3 days [cf. *Forbes et al.*, 2005; *Liu and Lühr*, 2005; *Sutton et al.*, 2005; *Bruinsma et al.*, 2006]. Here we adopt a uniform time span (2.5 days) to ensure that the mean values of the correlation and the corresponding optimal time (described below) are statistically meaningful, although it cannot completely capture the quiet, disturbed, and recovering states of the response of the density for all the storms. Because the two time series are on different time scales, the solar wind data corresponding to the time scale of the density are interpolated for present analysis. The resolution of the density time series is about 1.5 h (i.e., the length of one

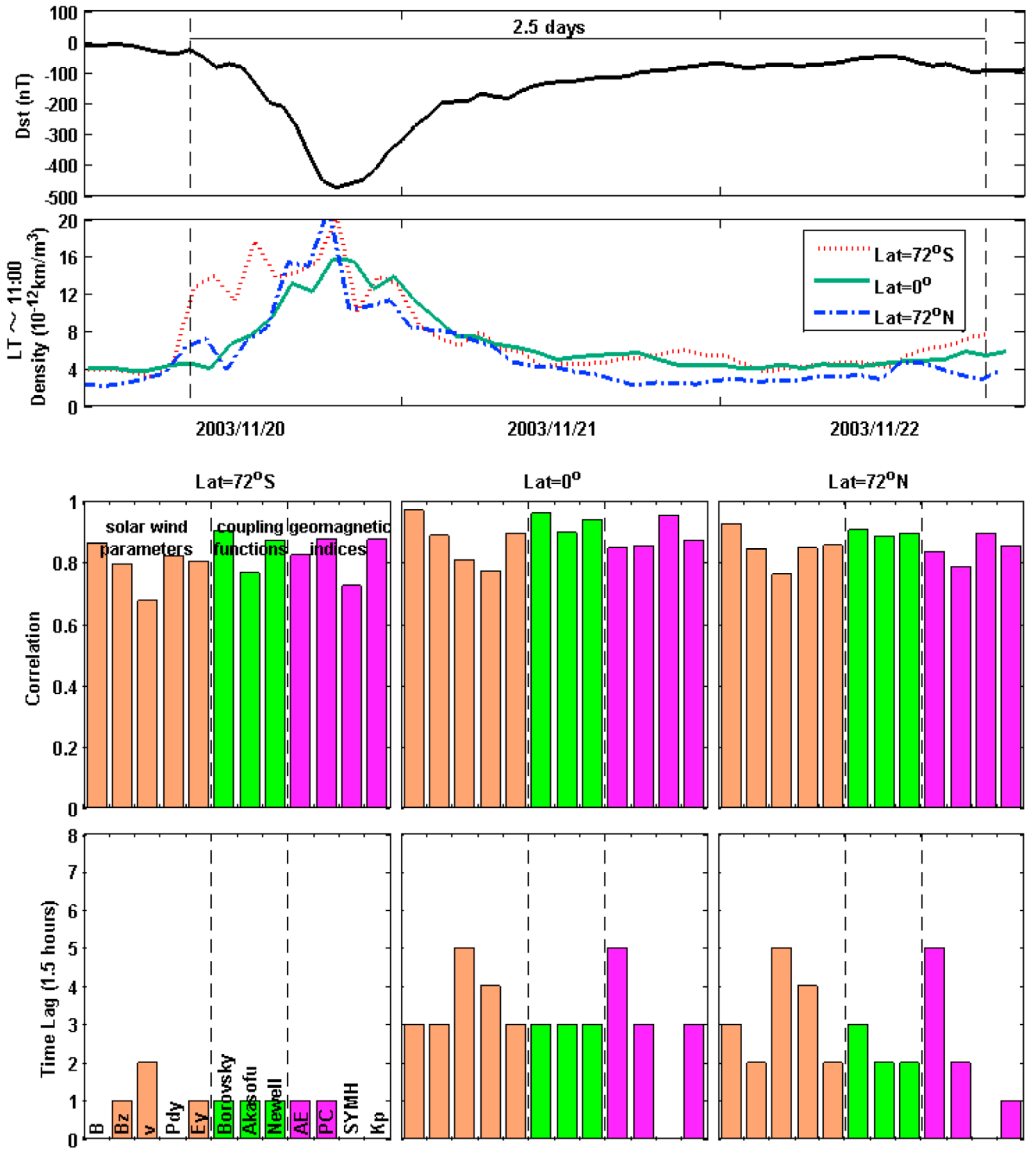

Figure 1. (top two panels) The Dst index and thermosphere density at local time near 1100 h (at 72°S, 0°, and 72°N latitude) for a 3 day interval from 20 to 22 November 2003; two dashed vertical lines mark the onset of the storm and the end time of the 2.5 days time span, respectively. (bottom two panels) Linear correlation coefficients and lag times between the various parameters or indices and density variations during the 2.5 days time span.

satellite orbit). To investigate the time lag of the density response, correlations at different time lags are computed between the density and solar wind data. Thus, we can find out the optimal time lag that corresponds to the best correlation. Then, the average correlation coefficients and corresponding optimal time lags are calculated to arrive at statistical results for the 52 storms.

3. Results

3.1. Solar Wind Parameters and Density Correlations

[11] Different solar wind parameters including coupling functions have turned out to have better or worse correlations during different geomagnetic storms. We illustrate this by comparing the correlations of the solar wind parameters and the density during four different storm events. In addition, four geomagnetic indices are also investigated for the purpose of comparison to the solar wind data results. They are the auroral electrojet index *AE*, the northern hemisphere polar cap index PC (at Thule), the symmetric current index SYMH, and the *Kp* index. From top to bottom in Figures 1, 2, 3, and 4 are *Dst*, thermosphere density (at 72°S, 0°, and 72°N latitude), linear correlation coefficients and optimal time lags. Two dashed vertical lines in the top two panels mark the onset of the storm and the end time of the 2.5 days time span, respectively.

[12] Figure 1 shows an example of a storm that occurred on 20–22 November 2003. The minimum value of the *Dst* index (−472 nT) was reached at 2100 UT on 20 November. Pronounced density enhancements at local time near 1100 h

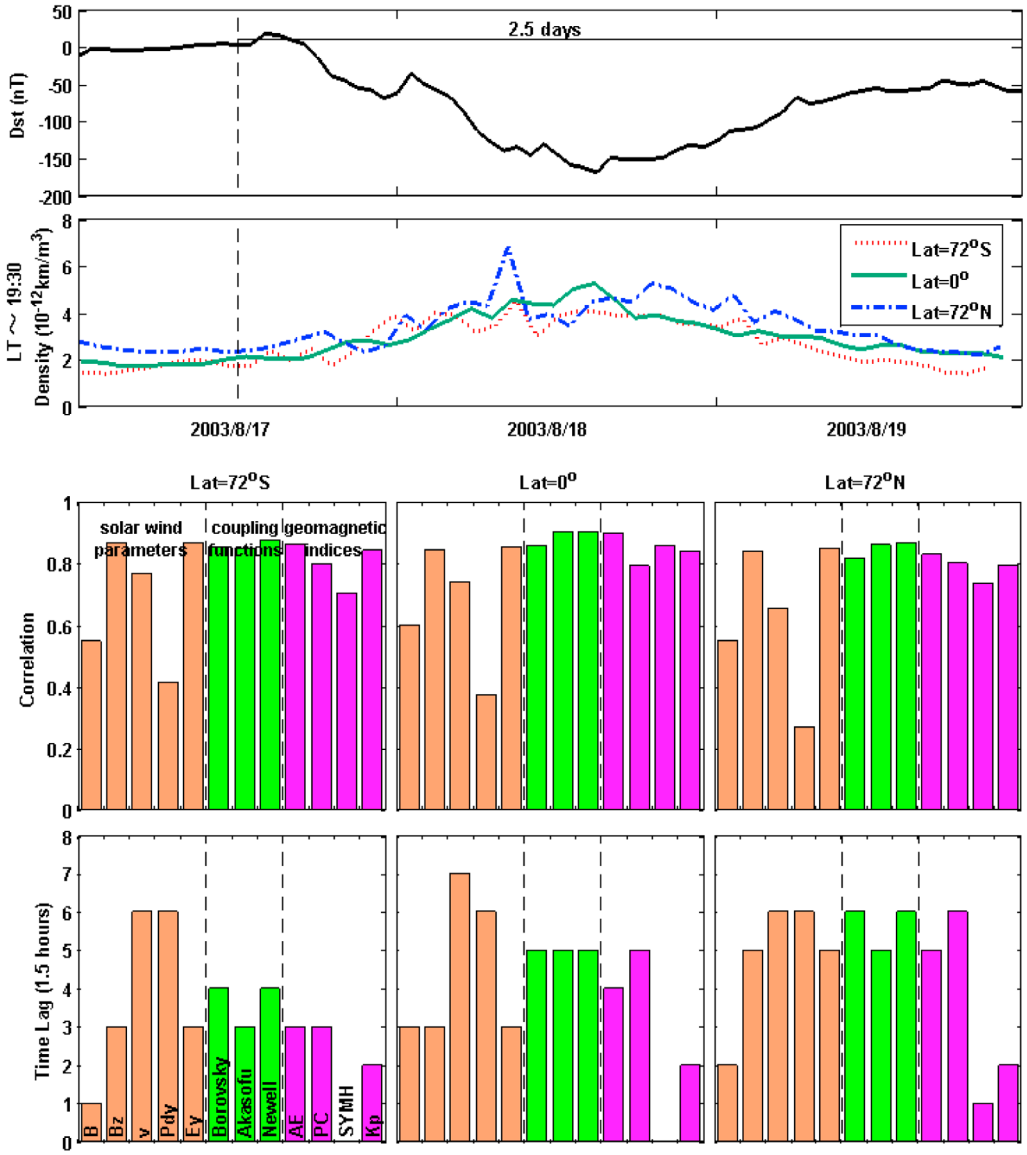

Figure 2. Same as Figure 1, but for thermosphere density at local time near 1930 h during the period 17–19 August 2003.

following the onset of the storm were observed. Furthermore, the enhancements occurred earlier at high latitude than at the equator. Among the chosen solar wind parameters (*B*, *Bz*, *v*, *Pdy*, and *Ey*), the magnetic field strength *B* shows the highest correlations with the density variations at high latitude and the equator. Moreover, *B* has better correlation with the density than do the selected coupling functions and the geomagnetic indices at 0° and 72°N latitude, whereas the Borovsky parameter shows the highest correlations with the density at 72°S latitude.

[13] Figure 2 presents an example of a storm that occurred on 17–19 August 2003. The minimum value of the *Dst* index (−148 nT) was reached at 1600 UT on 18 August. At 72°S latitude, *Bz*, *Ey*, and the Newell parameter show higher correlations with the density at local time near 1930 h, whereas the Akasofu parameter, the Newell parameter and *AE* show higher correlations at the equator, and *Bz*, *Ey*, the Akasofu parameter, and the Newell parameter show higher correlations at 72°N latitude.

[14] Figure 3 is an example of better correlation between *Pdy* and the density at local time near 0300 h. This storm occurred on 29–31 May 2003, and the minimum value of the *Dst* index (−144 nT) was reached at 0200 UT on 30 May. The density at the equator exhibited much smoother and smaller enhancements, in contrast to the strong disturbances at high latitudes. *Pdy* shows the higher correlations with the density at 0° and 72°S latitude, whereas *Bz* and the Borovsky parameter exhibit slightly better correlations at 72°N latitude.

[15] Figure 4 is an example of the highest correlation between the *Kp* index and the density at local time near 1950 h. This storm occurred on 29–31 May 2005, and the minimum value of the *Dst* index (−138 nT) was reached at 1000 UT on 30 May. The density at the equator exhibited much smoother and smaller enhancements, in contrast to the strong disturbances at high latitudes. Among the chosen

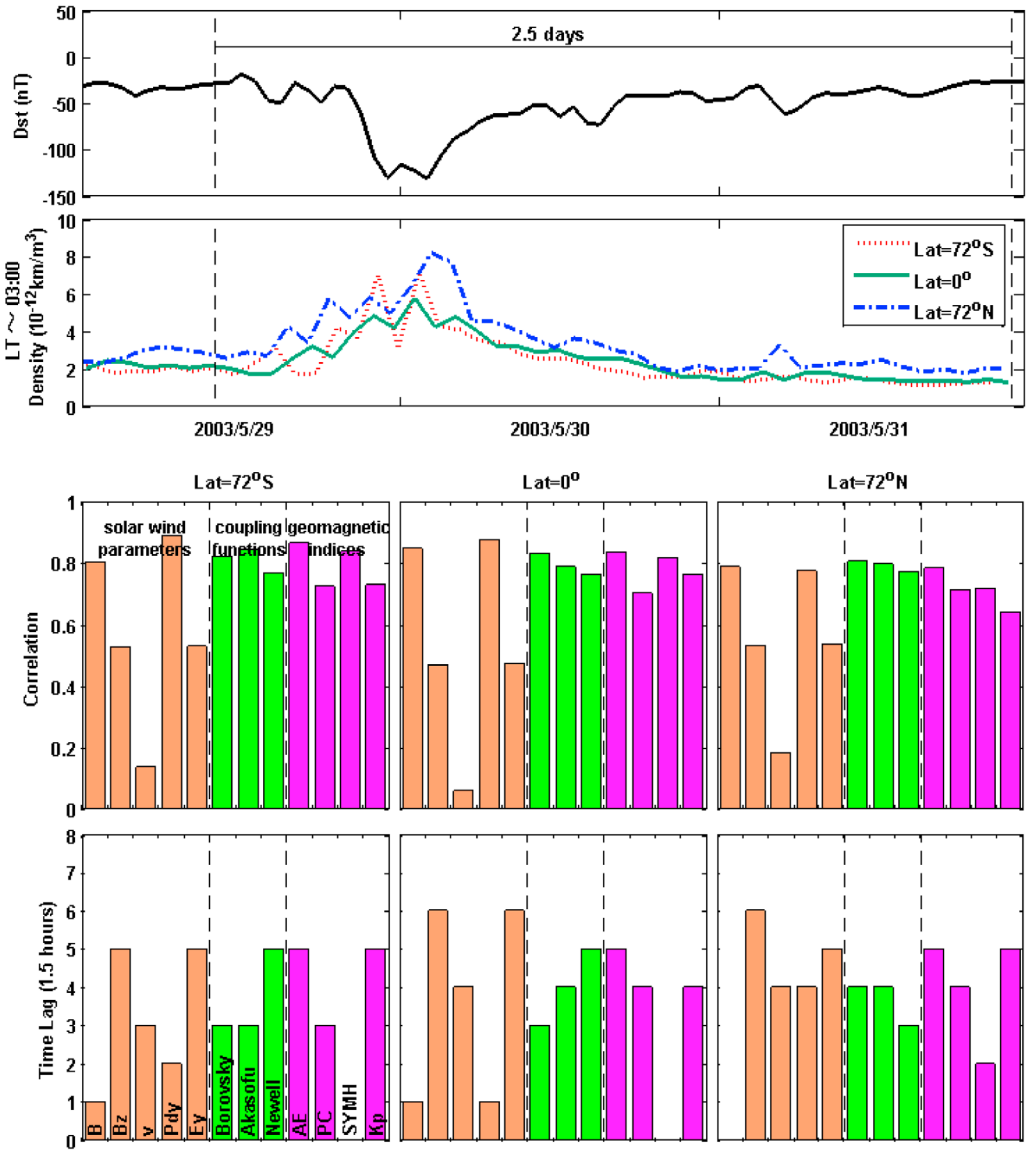

Figure 3. Same as Figure 1, but for thermosphere density at local time near 0300 h during the period 29–31 May 2003.

solar wind parameters and coupling functions, the Akasofu parameter shows the highest correlations with the density. However, it is worse correlated with the density than the *Kp* index except at 72°N latitude, where they show the comparable correlations with the density.

3.2. Statistical Results

[16] Examples such as those presented above suggest that different solar wind parameters show better or worse correlations during different geomagnetic storms. To find out the optimal solar wind parameters representing the energy input into the thermosphere, we have statistically analyzed the correlations between the solar wind parameters and the density for the 52 storms. Similarly, those four geomagnetic indices are also investigated for the purpose of comparison to the solar wind data results.

[17] Each orbit of the CHAMP satellite can be split into ascending and descending halves. During the period of each storm, the ascending orbit sampling is on the dayside or nightside, and the descending orbit sampling is on the opposite side. For the 52 storms studied, the average values of the correlations between the density (at 72°S, 0°, and 72°N latitude) and the solar wind parameters (*B*, *Bz*, *v*, *Pdy*, and *Ey*), the Borovsky parameter, the Akasofu parameter, the Newell parameter, and those four geomagnetic indices, together with the corresponding optimal time lags are illustrated in Figures 5 and 6 for dayside and nightside, respectively.

[18] As we can see from Figures 5 and 6, among the chosen solar wind parameters, the magnetic field strength *B* shows the highest correlations with the density for both dayside and nightside. As expected, the selected coupling functions, combining various solar wind parameters, have significantly better correlations with the density than does any one of the independent solar wind variables. The Borovsky parameter shows nearly the same correlations as the Akasofu parameter at high latitudes, whereas at the equator it exhibits better

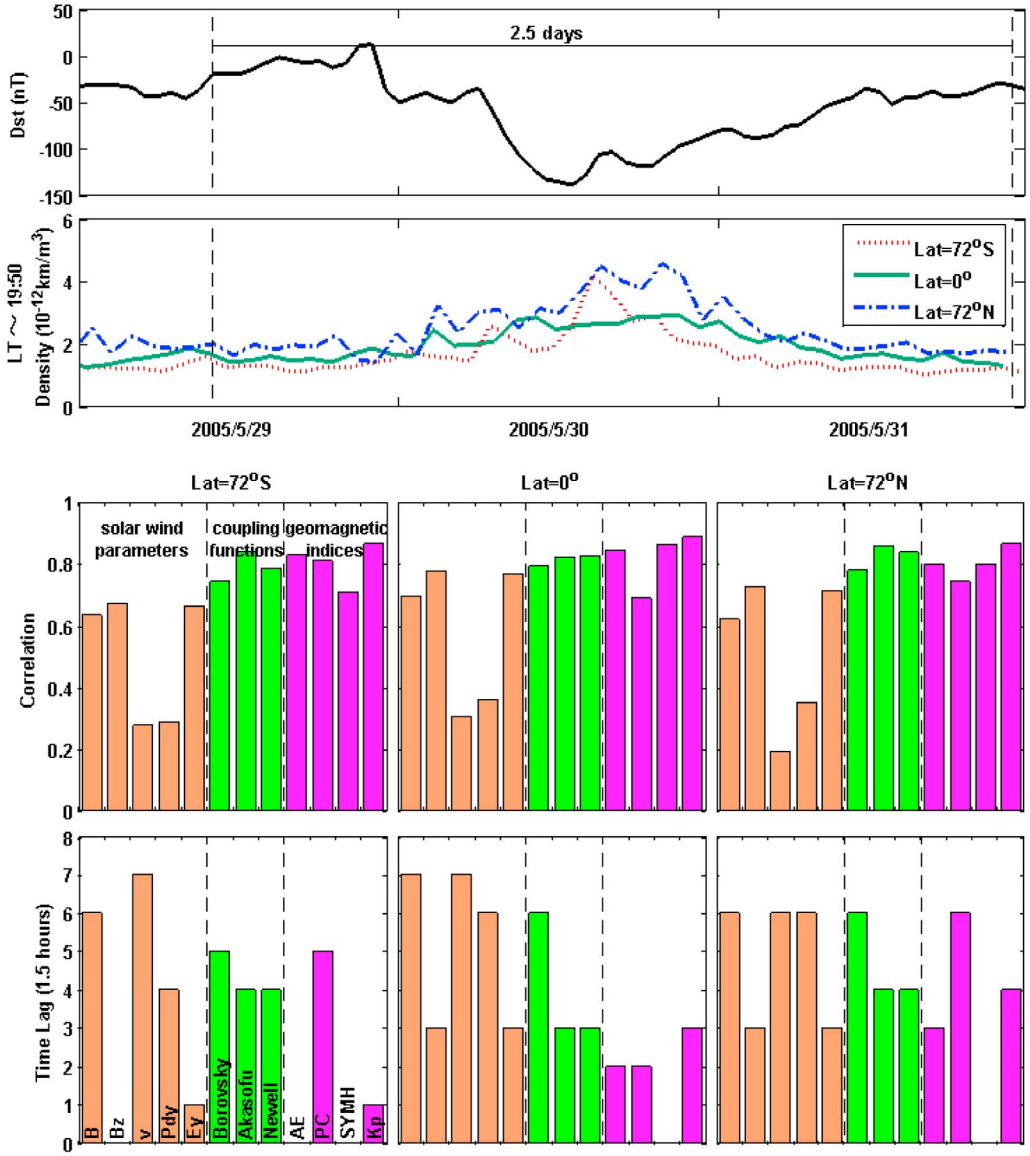

Figure 4. Same as Figure 1, but for thermosphere density at local time near 1950 h during the period 29–31 May 2005.

correlations than the Akasofu parameter, with the Newell parameter always close behind for both dayside and nightside. Among the four geomagnetic indices, the *AE* index shows the highest correlations with the density at high latitudes, whereas at the equator the *Kp* index shows the largest correlations for both dayside and nightside. For both dayside and nightside, the largest correlations for the geomagnetic indices are generally smaller (larger) than the corresponding correlations for the coupling functions (the solar wind parameters). On the other hand, for some chosen solar wind parameters and geomagnetic indices, the density lag times at the equator are longer than that at high latitude for both dayside and nightside. This is physically consistent with a disturbance that is initiated at high latitudes and propagates equatorward.

[19] As described above, the Borovsky parameter shows the best correlations with the density. Therefore, it is the preferred parameter for providing a quantitative assessment of the relationship between solar wind energy input and density variations. A summary of the quantitative results is given in Table 1. The correlations ($R \sim 0.80$) at the equator are significantly higher than those at high latitudes ($R \sim 0.69$–0.70 at 72°S latitude; $R \sim 0.69$–0.72 at 72°N latitude). Furthermore, it is interesting to note that the correlations on the dayside are almost the same as those on the nightside at 72°S and 0° latitude, whereas the correlation on the nightside is slightly higher than that on the dayside at 72°N latitude. On the other hand, the density lag times are shorter on the dayside as opposed to the nightside, with differences of about 1.5 h.

4. Discussion and Conclusions

[20] In this study, we have quantitatively assessed the relationship between solar wind parameters and density variations under strong disturbed conditions. It should be noted that the correlations may vary from event to event

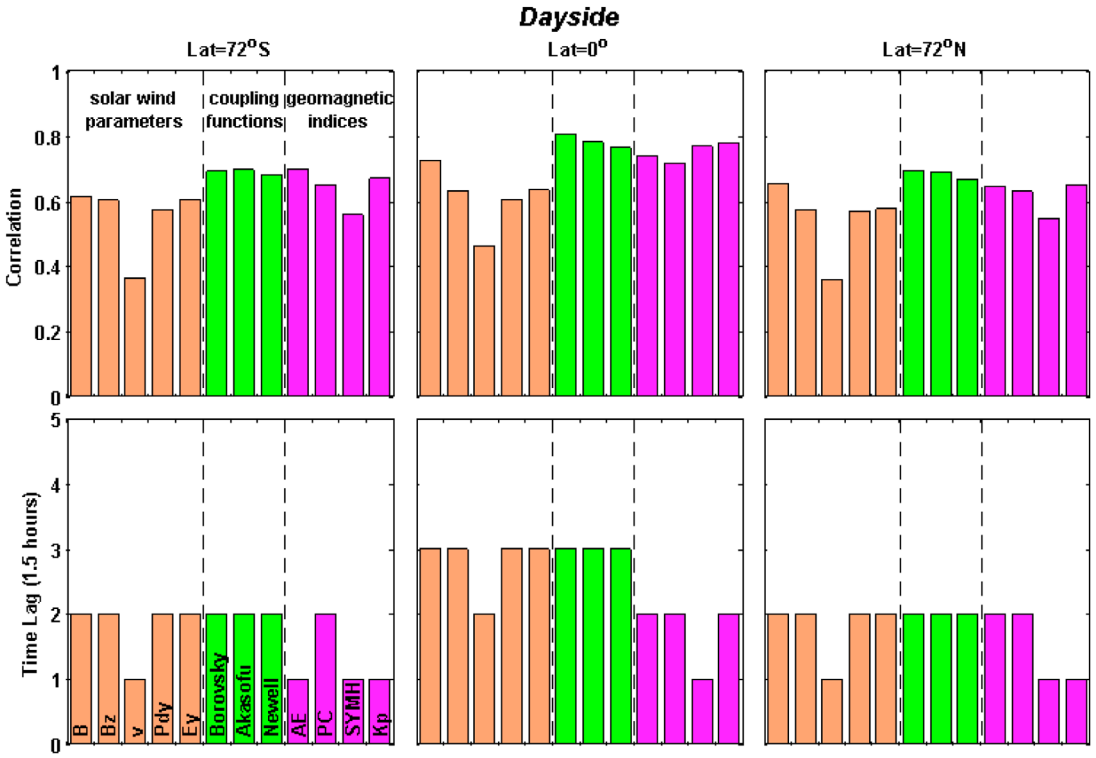

Figure 5. The average values of the correlations between the density on the dayside (at 72°S, 0°, and 72°N latitude) and solar wind parameters, coupling functions, and geomagnetic indices, and the corresponding optimal time lags for the 52 storms studied.

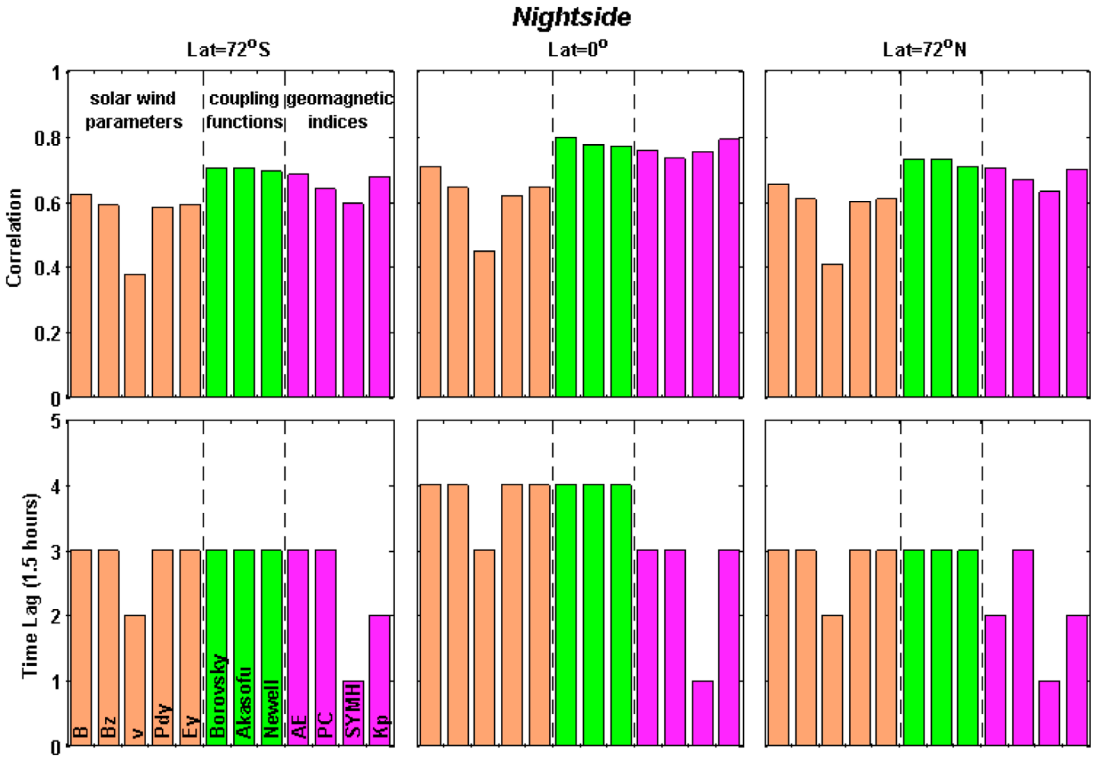

Figure 6. Same as Figure 5, but for the density on the nightside.

Table 1. Linear Correlation Coefficients and Lag Times Between the Borovsky Parameter and Density Variations at 72°S, 0°, and 72°N Latitude

Linear Correlation	Latitude = 72°S		Latitude = 0°		Latitude = 72°N	
	Dayside	Nightside	Dayside	Nightside	Dayside	Nightside
R	0.69	0.70	0.80	0.80	0.69	0.72
Lag (h)	3.0	4.5	4.5	6.0	3.0	4.5

owing to the effects associated with seasonal, local time (satellite sampling), solar cycle variations, as well as the "preconditioning" of the thermosphere. To examine the preconditioning effects on the statistical results, a mean background density defined according to the density fit using solar irradiance indices is removed [see *Guo et al.*, 2007], then the correlation analysis was done again between solar wind data and the density variations. The statistical results for the density without background (not shown) are very similar to those presented in Figures 5 and 6. Thus, we believe that the effects noted above would not make a great impact on our statistically results based on 52 storm events, especially the result that the Borovsky parameter correlates best with the global scale density variations.

[21] The correlations at the equator are significantly higher than those at high latitudes. This feature is possibly due to wind and temperature effects. Joule heating and particle precipitation are deposited in the high-latitude thermosphere, resulting in heating and expansion of the neutral gas. The kinetic energy of the neutral wind can be large locally sometimes. In addition, the vertical motion of neutral gas can cause the depletion in O/N_2 significantly at high latitudes and then the increase of mean molecular weight can offset the increase of neutral temperature [*Lei et al.*, 2010]. Therefore, the density enhancement does not always correspond to higher neutral temperature (i.e., local heating) [see *Lei et al.*, 2010]. Thus, wind and temperature effects may explain a higher correlation at the equator than at high latitudes sometimes. One other possible explanation is that the correlation at low latitudes may be affected by the more smooth density response at low latitudes, as opposed to the more variability over short time scales at high latitudes. Referring back to the examples shown in Figures 3 and 4, the density at the equator exhibited much smoother and smaller enhancements, in contrast to the strong disturbances at high latitudes.

[22] For the Borovsky parameter, on the dayside (nightside), the density lag time at the equator is about 4.5 (6.0) h, as compared with about 3.0 (4.5) h lag at 72°S and 72°N latitude. The 3 h time lag at high latitudes is consistent with processes controlling local density variations [*Ponthieu et al.*, 1988; *Burns et al.*, 1992], whereas the 4.5 h delay at the equator is consistent with interpretation in terms of large-scale traveling atmospheric disturbances [*Burns and Killee*, 1992; *Bruinsma and Forbes*, 2009]. The density lag times are generally shorter on the dayside than those on the nightside. This is not expected from simulations of *Fuller-Rowell et al.* [1996], who predict that the equatorward propagation of the density disturbance on the nightside is faster and more efficient than on the dayside. Their explanation was that on the nightside, the storm time density bulge at high latitudes encounters equatorward winds associated with the diurnal thermospheric tide, while on the dayside, it encounters poleward winds. As suggested by *Liu and Lühr* [2005], one possible explanation for our result is that the equatorward wind produced by the storm time density gradient at high latitudes is much larger (double) on the dayside than on the nightside. It could thus overcome the poleward wind on the dayside, leading to a faster propagation than on the nightside. On the other hand, the advection of energy away from its source should cause the observed lag times to increase with increasing distance from a source of energy.

[23] In conclusion, correlations between the thermosphere density variations and various solar wind parameters and coupling functions representing the energy input into the thermosphere reveal significantly different characteristics during different geomagnetic storms. Statistical analysis shows that, out of the chosen solar wind parameters including coupling functions, the Borovsky parameter correlates best with the global scale density variations. The correlations at the equator are significantly higher than those at high latitudes. Moreover, the correlations on the dayside are almost the same as those on the nightside at 72°S and 0° latitude, whereas the correlation on the nightside is slightly higher than that on the dayside at 72°N latitude. Our results indicate that it might be possible to use solar wind measurements to improve advance predictions of thermosphere density perturbations and the resulting changes in satellite drag, although the predictions are quantitatively rather crude due to the dependence of the global scale geomagnetic response on season, local time, solar cycle, etc.

[24] **Acknowledgments.** CHAMP is managed by the GeoForschungsZentrum (GFZ), Potsdam, Germany. The OMNI solar wind data base is compiled by the Space Physics Data Facility at the Goddard Space Flight Center. The polar cap data were provided by the Danish Meteorological Institute. The geomagnetic data (Dst, SYMH, AE, Kp) are provided by the World Data Center for Geomagnetism at Kyoto University. This work is jointly supported by the National Natural Science Foundation of China (40890162, 40921063, 41004082, and 40904049), 973 Program under grant 2006CB806304, the Knowledge Innovation Program of the Chinese Academy of Sciences, the Specialized Research Fund for State Key Laboratories, the National Science Foundation for Postdoctoral Scientists of China, AFOSR MURI award FA9550-07-1-0565 to the University of Colorado, and Collaborating Research Program of Key Laboratory of Solar Activity, National Astronomical Observatories, Chinese Academy of Sciences.

[25] Bob Lysak thanks Alan Burns for his assistance in evaluating this paper.

References

Akasofu, S.-I. (1981), Energy coupling between the solar wind and the magnetosphere, *Space Sci. Rev.*, *28*, 121–190.

Borovsky, J. E. (2008), The rudiments of a theory of solar wind/magnetosphere coupling derived from first principles, *J. Geophys. Res.*, *113*, A08228, doi:10.1029/2007JA012646.

Bowman, B. R., and W. K. Tobiska (2006), Improvements in modeling thermospheric densities using new EUV and FUV solar indices, paper presented at Spaceflight Mechanics Meeting, Am. Astron. Soc., Am. Inst. Aeron. Astronaut., Tampa, Fla.

Bruinsma, S. L., and J. M. Forbes (2009), Properties of traveling atmospheric disturbances (TADs) inferred from CHAMP accelerometer observations, *Adv. Space Res.*, *43*, 369–376, doi:10.1016/j.asr.2008.10.031.

Bruinsma, S., J. M. Forbes, R. S. Nerem, and X. Zhang (2006), Thermosphere density response to the 20–21 November 2003 solar and geomagnetic storm from CHAMP and GRACE accelerometer data, *J. Geophys. Res.*, *111*, A06303, doi:10.1029/2005JA011284.

Burns, A. G., and T. L. Killee (1992), The equatorial neutral thermospheric response to geomagnetic, *Geophys. Res. Lett.*, *19*(10), 977–980, doi:10.1029/92GL00522.

Burns, A. G., T. L. Killeen, and R. G. Roble (1992), Thermospheric heating away from the auroral oval during geomagnetic storms, *Can. J. Phys.*, *70*, 544–552.

Forbes, J. M., R. G. Roble, and F. A. Marcos (1987), Thermospheric dynamics during the March 22, 1979, magnetic storm: 2. Comparisons of model predictions with observations, *J. Geophys. Res.*, *92*(A6), 6069–6081, doi:10.1029/JA092iA06p06069.

Forbes, J. M., R. Roble, and F. A. Marcos (1993), Magnetic activity dependence of high-latitude thermospheric winds and densities below 200 km, *J. Geophys. Res.*, *98*(A8), 13,693–13,702, doi:10.1029/93JA00155.

Forbes, J. M., R. Gonzalez, F. A. Marcos, D. Revelle, and H. Parish (1996), Magnetic storm response of lower thermosphere density, *J. Geophys. Res.*, *101*(A2), 2313–2319, doi:10.1029/95JA02721.

Forbes, J. M., G. Lu, S. Bruinsma, S. Nerem, and X. Zhang (2005), Thermosphere density variations due to the 15–24 April 2002 solar events from CHAMP/STAR accelerometer measurements, *J. Geophys. Res.*, *110*, A12S27, doi:10.1029/2004JA010856.

Fuller-Rowell, T. J., M. V. Codrescu, H. Rishbeth, R. J. Moffett, and S. Quegan (1996), On the seasonal response of the thermosphere and ionosphere to geomagnetic storms, *J. Geophys. Res.*, *101*(A2), 2343–2353, doi:10.1029/95JA01614.

Guo, J., W. Wan, J. M. Forbes, E. Sutton, R. S. Nerem, T. N. Woods, S. Bruinsma, and L. Liu (2007), Effects of solar variability on thermosphere density from CHAMP accelerometer data, *J. Geophys. Res.*, *112*, A10308, doi:10.1029/2007JA012409.

Guo, J., W. Wan, J. M. Forbes, E. Sutton, R. S. Nerem, and S. Bruinsma (2008), Interannual and latitudinal variability of the thermosphere density annual harmonics, *J. Geophys. Res.*, *113*, A08301, doi:10.1029/2008JA013056.

Guo, J., X. Feng, J. Zhang, P. Zuo, and C. Xiang (2010), Statistical properties and geoefficiency of interplanetary coronal mass ejections and their sheaths during intense geomagnetic storms, *J. Geophys. Res.*, *115*, A09107, doi:10.1029/2009JA015140.

Koskinen, H. E. J., and E. Tanskanen (2002), Magnetospheric energy budget and the epsilon parameter, *J. Geophys. Res.*, *107*(A11), 1415, doi:10.1029/2002JA009283.

Lei, J., J. P. Thayer, A. G. Burns, G. Lu, and Y. Deng (2010), Wind and temperature effects on thermosphere mass density response to the November 2004 geomagnetic storm, *J. Geophys. Res.*, *115*, A05303, doi:10.1029/2009JA014754.

Liu, H., and H. Lühr (2005), Strong disturbance of the upper thermospheric density due to magnetic storms: CHAMP observations, *J. Geophys. Res.*, *110*, A09S29, doi:10.1029/2004JA010908.

Newell, P. T., T. Sotirelis, K. Liou, C.-I. Meng, and F. J. Rich (2007), A nearly universal solar wind-magnetosphere coupling function inferred from 10 magnetospheric state variables, *J. Geophys. Res.*, *112*, A01206, doi:10.1029/2006JA012015.

Ponthieu, J.-J., T. L. Killeen, K.-M. Lee, and G. R. Carignan (1988), Ionosphere-thermosphere momentum coupling at solar maximum and solar minimum from DE-2 and AE-C data, *Phys. Scr.*, *37*, 447–454.

Prölss, G. W. (1980), Magnetic storm associated perturbations of the upper atmosphere: Recent results obtained by satellite-borne gas analyzers, *Rev. Geophys.*, *18*(1), 183–202, doi:10.1029/RG018i001p00183.

Reigber, C., H. Lühr, and P. Schwintzer (2002), CHAMP mission status and perspectives, *Eos Trans. AGU*, *81*, 48.

Sutton, E. K. (2008), Effects of solar disturbances on the thermosphere densities and winds from CHAMP and GRACE satellite accelerometer data, Ph.D. dissertation, Univ. of Colo., Boulder.

Sutton, E. K., J. M. Forbes, and R. S. Nerem (2005), Global thermospheric neutral density and wind response to the severe 2003 geomagnetic storms from CHAMP accelerometer data, *J. Geophys. Res.*, *110*, A09S40, doi:10.1029/2004JA010985.

Sutton, E. K., J. M. Forbes, and D. J. Knipp (2009), Rapid response of the thermosphere to variations in Joule heating, *J. Geophys. Res.*, *114*, A04319, doi:10.1029/2008JA013667.

Tobiska, W. K., S. D. Bouwer, and B. R. Bowman (2006), The development of new solar indices for use in thermospheric density modeling, paper presented at Astrodynamics Specialist Conference and Exhibit, Am. Inst. Aeron. Astronaut., Am. Astron. Soc., Keystone, Colo.

Wilson, G. R., D. R. Weimer, J. O. Wise, and F. A. Marcos (2006), Response of the thermosphere to Joule heating and particle precipitation, *J. Geophys. Res.*, *111*, A10314, doi:10.1029/2005JA011274.

Zhang, J., et al. (2007), Solar and interplanetary sources of major geomagnetic storms (Dst ≤ -100 nT) during 1996–2005, *J. Geophys. Res.*, *112*, A10102, doi:10.1029/2007JA012321.

Zhang, J., I. G. Richardson, and D. F. Webb (2008), Interplanetary origin of multiple-dip geomagnetic storms, *J. Geophys. Res.*, *113*, A00A12, doi:10.1029/2008JA013228.

X. Feng and J. Guo, SIGMA Weather Group, State Key Laboratory of Space Weather, CSSAR, Chinese Academy of Sciences, Beijing 100190, China. (fengx@spaceweather.ac.cn; jpguo@spaceweather.ac.cn)

J. M. Forbes and J. Lei, Department of Aerospace Engineering Sciences, University of Colorado at Boulder, Boulder, CO 80309, USA. (forbes@colorado.edu; jiuhou.lei@colorado.edu)

C. Tan, Key Laboratory of Solar Activity, National Astronomical Observatories, Chinese Academy of Sciences, Beijing 100012, China. (tanchm@nao.cas.cn)

J. Zhang, Department of Computational and Data Sciences, George Mason University, 4400 University Dr., MSN 6A2, Fairfax, VA 22030, USA. (jzhang7@gmu.edu)